A novel UV pumped yellow-emitting phosphor $Ba_2YAlO_5:Dy^{3+}$ for white light-emitting diodes

Bin Deng[1,2*], Jun Chen[1,2], Chong-song Zhou[1,2] and Hui Liu[1,2]

[1]College of Chemistry & Biology and Environmental Engineering, Xiangnan University, Chenzhou 423043, Hunan, P. R. China;
[2] Hunan Provincial Key Laboratory of Xiangnan Rare-Precious Metals Compounds Research and Application, Chenzhou 423043, Hunan, P. R. China;

Abstract. A series of novel Dy^{3+} activated aluminate $Ba_2Y_{1-x}Dy_xAlO_5$ (x = 0.01–0.30) red-emitting phosphors were synthesized through a high-temperature solid-state route at 1380°C. The X-ray diffraction patterns revealed that the samples were well crystallized in the space group $P2_1/c$ (No. 14). The spectrum analysis revealed that under UV light excitation, $Ba_2YAlO_5:Dy^{3+}$ phosphor exhibited blue and yellow peaks corresponding to $^4F_{9/2}$–$^6H_{15/2}$ transition and $^4F_{9/2}$–$^6H_{13/2}$ transition, respectively. The optimum dopant concentration of Dy^{3+} ions is around 2 mol% and the critical transfer distance of Dy^{3+} is calculated as 29 Å. The concentration quenching mechanism between Dy^{3+} has been investigated. Results indicate that $Ba_2YAlO_5:Dy^{3+}$ offers the excellent optical properties as a potential yellow-emitting phosphor candidate for n-UV LEDs.

1 Introduction

Dy^{3+} as the activator can be doped into suitable hosts to obtain white light emission in a single phase. It can present two characteristic emission bands in luminescence spectrum, $^4F_{9/2}\rightarrow{}^6H_{15/2}$ at 488 nm (blue) and $^4F_{9/2}\rightarrow{}^6H_{13/2}$ at 580 nm (yellow)[1, 2]. The feasibility of the phosphor to generate white light is actually indicated by the Yellow and Blue (Y/B) ratios [3].

Recently, white light-emitting diodes (WLEDs) have gained enormous interest from scientists and engineers as a promising light source, which are important candidates for solid-state lighting due to its high luminous efficiency, compactness, long-lifetime, diversity design, fast switching material stability and environmental friendly [4, 5]. LEDs are regarded as environmentally friendly because they have not utilized the toxic elements such as mercury (excitation light source) and colloidal cadmium selenide quantum dots. The most commercially available w-LEDs are fabricated by a combination of InGaN LED chips with $Y_3Al_5O_{12}:Ce^{3+}$ yellow-emitting phosphor [1]. But the above method infers some major disadvantages in the red spectral region, including correlated color temperature that is higher than 4500 K and color rendering index that is lower than 80. Another effective method is to utilize near-UV LEDs chips coupled with multi-phosphors of red, green and blue phosphor [6, 7].

The aluminates have been extensively explored as hosts for phosphors due to their excellent optical properties [8, 9]. In this paper, we report the red emitting phosphors $Ba_2Y_{1-x}Dy_xAlO_5$ (x = 0.01–0.30) under NUV (Near Ultraviolet) excitation. The phase purity, photoluminescence (PL) properties, influence of doping concentration, and chromaticity coordinate of the $Ba_2YAlO_5:Dy^{3+}$ phosphors were investigated.

2 EXPERIMENTAL PROCEDURE

The synthesis of powder samples $Ba_2Y_{1-x}Dy_xAlO_5$ (x = 0.01, 0.02, 0.05, 0.10, 0.15, 0.20, 0.25, and 0.30) phosphors with the concentration of Dy^{3+} from 1 to 30 mol% was carried out by conventional solid stated reaction in air. Al_2O_3 (nanopowder, A.R.), $BaCO_3$ (A.R.), Y_2O_3 (99.99%), and Dy_2O_3 (99.99%) were completely mixed and ground in an agate mortar. Then the mixtures were put into an alumina crucible and preheated at 600 °C in air for 3 h. After that, the samples were reground completely and calcined in air at 1380 °C for 5 h. The associated reaction equations are as follows:

$$4BaCO_3 + (1\text{-}x)Y_2O_3 + Al_2O_3 + xDy_2O_3 \xrightarrow{1380℃\times 5h} 2Ba_2Y_{1-x}Dy_xAlO_5 + \text{volatile products}$$

X-ray powder diffraction (XRD) was performed with Philips X'Pert MPD (Philips, Netherlands) with Cu Kα radiation (λ = 1.5418 Å) to identify the phase purity of the as-prepared samples. Data collection was carried out in the range of 2θ = 10°−70°. Luminescence properties of the synthesized phosphors were performed using FLS 920 spectrometer (Edinburgh) at room temperature.

3 RESULTS AND DISCUSSION

* Corresponding author: dengbinxnu@163.com (Bin Deng)

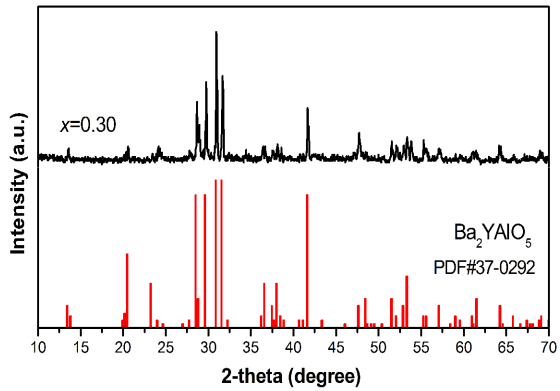

Fig. 1. XRD pattern of the representative $Ba_2Y_{0.98}Dy_{0.02}AlO_5$ phosphor

The phase purity of the Ba_2YAlO_5:0.02Dy^{3+} phosphors are identified by XRD and depicted in Fig. 1. All the diffraction peaks of the sample were consistent with the standard card (No.37-0292) for the Ba_2YAlO_5. The lattice constants of Ba_2YAlO_5:0.02Dy^{3+} are calculated to be a = 13.1702 Å, b = 7.4539 Å, c = 5.7102 Å and V = 527.22 $Å^3$, respectively. It suggests that the Dy^{3+} ions substituted the Y^{3+} sites in Ba_2YAlO_5 due to their similar ionic radii of Dy^{3+} (r = 0.912 Å) and Y^{3+} (0.900 Å) when coordination number = 6 [10].

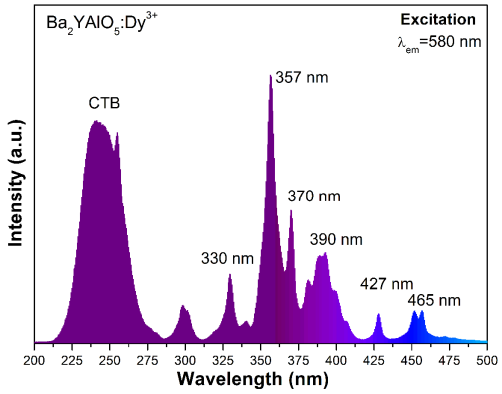

Fig. 2. Excitation spectrum of Ba_2YAlO_5:0.02Dy^{3+} phosphor (λ_{em} = 580 nm).

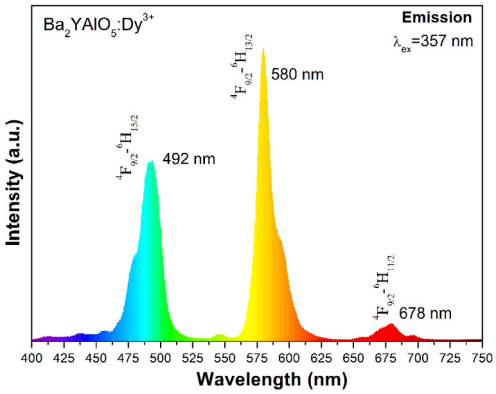

Fig. 3. Emission spectrum of Ba_2YAlO_5:0.02Dy^{3+} phosphor (λ_{ex} = 357 nm).

Fig. 2 depicts the excitation spectrum of Ba_2YAlO_5:0.02Dy^{3+} phosphor when recorded at 580 nm. The broad excitation band (~242 nm) is ascribed to the host absorption of the O^{2-}→Dy^{3+} ions charge-transfer band (CTB) [11, 12]. The sharp PLE peaks were observed in the range between 280 and 500 nm are assigned to *f–f* transition of Dy^{3+} ions [13]. The main excitation band centered at 330, 370, 390, 427 and 465 nm corresponding to the $^6H_{15/2} \rightarrow {}^6P_{3/2}$, $^6H_{15/2} \rightarrow {}^6P_{5/2}$, $^6H_{15/2} \rightarrow {}^4I_{11/2}$, $^6H_{15/2} \rightarrow {}^4G_{11/2}$ and $^6H_{15/2} \rightarrow {}^4I_{15/2}$ transition, respectively [14]. The peak at 357 nm is the strongest one which results from $^6H_{15/2}$→$^6P_{7/2}$ transition. Thus, the Ba_2YAlO_5:Dy^{3+} phosphors are suitable for InGaN-chip based w-LEDs.

The emission spectrum of Ba_2YAlO_5:0.02Dy^{3+} excited at 357 nm is shown in Fig. 3. The PL spectrum consists of four sharp lines in 450-750 nm attributing to the $^4F_{9/2}$→$^6H_{J/2}$ (J = 15, 13, 11, 9) transitions of Dy^{3+}, respectively. Three prominent emission bands centered associate with 492 nm (blue), 580 nm (yellow), and 678 nm (red). To our knowledge, $^4F_{9/2}$→$^6H_{13/2}$ transition of Dy^{3+} belongs to hypersensitive transitions. When Dy^{3+} is located at a low-symmetry local site, this emission transition dominates in emission spectra, and otherwise the blue emission is dominant [11, 15]. In the crystal structure of the Ba_2YAlO_5, Y^{3+} occupied 4e sites with six O atoms around them, forming [YO_6] octahedra. Y-O lengths are not the same and varied from 2.182 Å to 2.307 Å. Therefore, the Dy ions located in low symmetrical cationic environment when substitute the Y^{3+} ions. In this work, the yellow emission is the most intense, which mean that Dy^{3+} ions mainly located in a low-symmetrical cation environment.

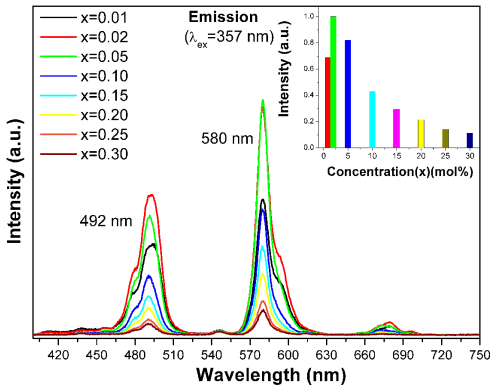

Fig. 4. The influence of the concentration on the emission intensity of $Ba_2Y_{1-x}Dy_xAlO_5$ phosphor (*x* = 0.01, 0.02, 0.05, 0.10, 0.15, 0.20, 0.25, and 0.30).

Figure 4 showed the concentration influences to the PL intensities of Ba_2YAlO_5:*x*Dy^{3+} phosphor (*x* = 0.01, 0.02, 0.05, 0.10, 0.15, 0.20, 0.25, and 0.30) phosphors (λ_{ex} = 357 nm). With different concentrations, there is no different shift in PL spectra. The insets demonstrate that the emission intensity increases with Dy^{3+} contents from *x* value of 1 mol%–2 mol%, thereafter decreases. The phosphor appeared concentration quenching phenomenon. Concentration quenching refers to any process which decreases the fluorescence intensity of a given substance as the doping concentration increases. A famous theory is presented for concentration quenching in solid systems, based on the migration of excitation energy from one activator center to another and eventually to an imperfection which may act as an energy sink [16]. The optimal doping concentration of Dy^{3+} ion is *x* = 2 mol%.

The critical energy transfer distance (R_c) between Dy^{3+} ions in $Ba_2Y_{1-x}Dy_xAlO_5$ phosphors can be evaluated by the following formula given by Blasse [17]:

$$R_c \approx 2\left(\frac{3V}{4\pi\, x_c N}\right)^{1/3} \qquad (1)$$

where *N* means the formula units per unit cell, x_c represents the critical concentration of Dy^{3+}, and *V* is the volume of the unit cell. Taking the appropriate values of *N*, *V*, and x_c(2, 526.48 $Å^3$, and 0.02, respectively) for the Ba_2YAlO_5:0.02Dy^{3+} phosphor, we estimate R_c to be about 29 Å, which is far greater than 5 Å. Thus, the concentration quenching mechanism of Dy^{3+} ions can be mainly ascribed to the multipole–multipole interaction.

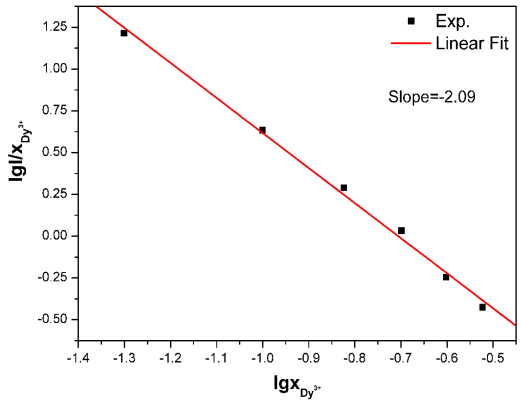

Fig. 5. Curve of lgI /x vs. lgx in Ba_2YAlO_5:xDy^{3+} phosphor (λ_{ex} = 357 nm).

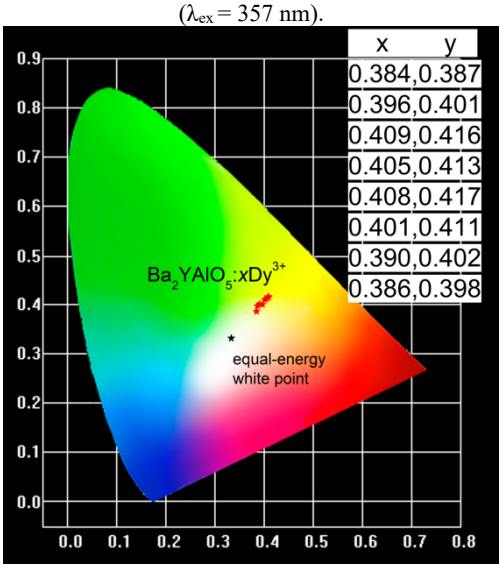

Fig. 6. CIE chromaticity coordinates for the Ba_2YAlO_5:xDy^{3+} sample.

Dexter theory identified non-radiative energy transition is caused by an exchange interaction or radiation reabsorption or multipole–multipole interaction. The relationship between emission intensity and activator concentration needs to be can be expressed by the following formula [18]:

$$\frac{I}{x} = K\left[1+\beta\left(x\right)^{Q/3}\right]^{-1} \qquad (2)$$

where χ is the dopant concentration; in given host, k and β are constants for each interaction at the same excitation condition; Q is index of electric multipole, including 6, 8, and 10 for the electric dipole-dipole, electric dipole-quadrupole, and electric quadrupole–quadrupole interaction, respectively [16]. Therefore, in this case, the correlation between lgI/x and lg$x$ is nearly linear and the slope parameter is obtained to be -2.09 as shown in Fig. 5. The slope of the linear fitting equaled to -θ/3, and then the value of θ was estimated approximately to be 6. Consequently, the result indicated that the energy transfer among the electric dipole-dipole interaction was dominated by the luminescence quenching of Dy^{3+} doped $Ba_2Y_{1-x}Dy_xAlO_5$ host.

The color-coordinate issue is indispensable in the evaluation of the phosphor performance. Therefore, the Commission International de I'Eclairage (CIE) chromaticity coordinates of Dy^{3+}-doped Ba_2YAlO_5 were calculated according to the PL spectra under 357 nm excitation. The chromaticity diagram of Ba_2YAlO_5:xDy^{3+} was presented with a red star in Fig. 6. The CIE chromaticity coordinate of the Ba_2YAlO_5:xDy^{3+}(x = 0.01, 0.02, 0.05, 0.10, 0.15, 0.20, 0.25, and 0.30) phosphors are (0.384, 0.387), (0.396, 0.401) (0.409, 0.416), (0.405, 0.413), (0.408, 0.417), (0.401, 0.411), (0.390, 0.402), and (0.386, 0.398), respectively. Clearly, all the color coordinates of samples located at the yellow light region in the CIE 1931 chromaticity diagram. Hence, Ba_2YAlO_5:Dy^{3+} phosphor could be considered as a potential yellow-emitting candidate for WLEDs under 357 nm excitation.

4 CONCLUSION

In summary, we have synthesized a series of aluminate yellow-emitting Ba_2YAlO_5:Dy^{3+} phosphors by a solid-state reaction. The XRD examined results confirmed that all the compounds crystallize in the space group $P2_1/c$ (14). The synthesized phosphors Ba_2YAlO_5:Dy^{3+} was excited by 357 nm, and showed a strong yellow-emitting emission at 580 nm which was assigned to the $^4F_{9/2}\rightarrow{}^6H_{13/2}$ transition of Dy^{3+} ions. When the doping concentration was over 2 mol%, the phosphor appeared concentration quenching phenomenon. The electric dipole-dipole interaction is the concentration quenching mechanism of Ba_2YAlO_5:Dy^{3+} phosphors. All the above properties indicated the Dy^{3+}-activated Ba_2YAlO_5 phosphors could be a new yellow-emitting candidate for color mixing in the white light-emitting diode.

Acknowledgment

The authors thank Hunan provincial key laboratory of Xiangnan rare-precious metals compounds and applications and the construct program of the key discipline in Hunan province for financial support.

References

1. B. Liu, C. Shi, Appl. Phys. Lett. **86**(19), 191111 (2009)
2. Q. Su, H. Liang, C. Li, H. He, Y. Lu, J. Li, Y. Tao, J. Lumin. **122,** (927 (2007)
3. Q. Su, Z. Pei, L. Chi, H. Zhang, Z. Zhang, F. Zou, J. Alloys Compd. **192**(1), 25 (1993)
4. Z. Xia, Q. Liu, Prog. Mater Sci. **84**(59 (2016)
5. P.F. Smet, A.B. Parmentier, D. Poelman, J. Electrochem. Soc. **158**(6), R37 (2011)
6. R.J. Xie, N. Hirosaki, Y. Li, T. Takeda, Materials **3**(6), 3777 (2010)
7. R. Yu, A. Fan, M. Yuan, T. Li, Q. Tu, J. Wang, Opt. Mater. Express **6**(7), 2397 (2016)
8. F.M. Emen, R. Altinkaya, V.E. Kafadar, G. Avsar, T. Yeşilkaynak, N. Kulcu, J. Alloys Compd. **681**(32), 260 (2016)
9. W. You, Z. Xiao, F. Lai, X. Ye, Q. Zhang, H. Jiang, C. Wang, J. Liao, X. Liu, S. Zhong, J. Mater. Sci. **51**(11), 1 (2016)
10. R.D. Shannon, Acta Crystallographica, Section A: Crystal Physics, Diffraction, Theoretical and General Crystallography **A32**(5), 751 (1976)
11. S. Liu, J. He, Z. Wu, J.H. Jeong, B. Deng, R. Yu, J. Lumin. **200**(164 (2018)

12. P. Dorenbos, J. Phys.: Condens. Matter **15**(49), 8417 (2003)
13. W.T. Carnall, P.R. Fields, K. Rajnak, J. Chem. Phys. **49**(10), 4424 (1968)
14. G. Lakshminarayana, H. Yang, J. Qiu, J. Solid State Chem. **182**(4), 669 (2009)
15. M. Yu, J. Lin, Z. Wang, J. Fu, S. Wang, H.J. Zhang, Y.C. Han, Chem. Mater. **14**(5), 2224 (2002)
16. D.L. Dexter, J.H. Schulman, J. Chem. Phys. **22**(6), 1063 (1954)
17. G. Blasse, B.C. Grabmaier, Springer-Verlag, Berlin, Heidelberg 46 (1994)
18. L.G. Van Uitert, J. Electrochem. Soc. **114**(10), 1048 (1967)